한국박용기관학회지 제28권, 제6호, pp. 906~915, 2004. 9 (ISSN 1226-9549)
Journal of the Korean Society of Marine Engineers

자기부상 스테이지의 모델링과 제어

남택근† · 김용주* · 전정우**

(원고접수일 : 2003년 12월 15일, 심사완료일 : 2004년 4월 21일)

Modeling of a Magnetic Levitation Stage and its Control

Taek-Kun Nam† · Yong-Joo Kim* and Jeong-Woo Jeon**

Abstract : In this paper, we address the development of magnetic levitation positioning system. This planar magnetic levitator employs four permanent magnet liner motors. Each motor generates vertical force for suspension against gravity, as well as horizontal force for driving levitation object called a platen. This stage can generate six degrees of freedom motion by the vertical and horizontal force. We derived the mechanical dynamics equation using Lagrangian method and used coenergy to express an electromagnetic force. We proposed a control algorithm for the position and posture control from its initial value to its desired value using sliding mode control. Some simulation results are provided to verify the effectiveness of the proposed control scheme.

Key words : Magnetic Levitation, Lagrangian, Co-energy, Sliding mode Control

1. Introduction

The importance of high precision positioning mechanism is increased with the high demand of advanced technologies delivering products with superior performance and good tolerance. We can easily found that the high precision positioning mechanisms play an important role in the field of modern fabrication process such as an ultra precision machining, precise alignment of optical device, and wafer steppers in semiconductor manufacturing. Such devices could support micro or even nano positioning accuracy, high bandwidths of operation, and sufficient stiffness. Piezoelectric actuators provide the necessary stiffness and positioning accuracy but have some restriction with

† 책임저자(Div. of Marine Eng., Mokpo National Maritime University), E-mail : tknam@mmu.ac.kr
* Machine control & Application Research Group, Korea Electrotechnology Research Institute, yjkim@keri.re.kr
** Machine control & Application Research Group, Korea Electrotechnology Research Institute , jwjeon@keri.re.kr

its traveling range. Use of mechanical bearings or cascading arrangements suffers from slow response and the presence of undesirable mechanical elements such as clearances and friction. The combination of linear motor and air-bearing is a general strategy to realize long stroke movement with high velocities. But to achieve a large and accurate travel in multiple degrees of freedom using linear motor with non-contact bearing, it needs complex system configuration. In contrast, the magnetic levitation is contact-less mechanism which enables high precision in positioning accuracy and multiple d.o.f (degrees of freedom) to be achieved without mechanical guide or compounding.

In the previous works for the control of magnetic levitation positioner, Cho [3] tackled position control of magnetic suspension actuator with one d.o.f using sliding mode control method. Mittal [6] addressed long travel motion control of a magnetic suspension actuator using a combination of feedback linearization technique and discrete-time delay compensation algorithm. Kim et al. developed a magnetic levitation stage with a six degree of freedom(6 DOF) [4].

We designed a magnetic levitation stage as the inferred result of Kim's [4]. The differences between Kim and our work are as follows. A linear approximation and lead-lag compensator was applied to control the magnetic levitation stage in Kim's work [4]. In our work, we derived a mechanical dynamics equation of the platen using Lagrangian equation and proposed configuration control algorithm using a sliding mode control method. The sliding mode control method can be applied to a nonlinear system in the global sense, and the performance and stability robustness to model uncertainty and disturbances could be achieved by control switching. Finally, we verified the effectiveness of the proposed control scheme from a numerical simulation.

2. System configuration

The magnetic levitation stage is shown in Fig. 1. This levitator is composed of four permanent magnet linear motors. Each motor generates vertical force for suspension against gravity and horizontal force for driving platen. The actuators for this magnetic levitator are three phase surface-wound surface-permanent magnet linear motors.

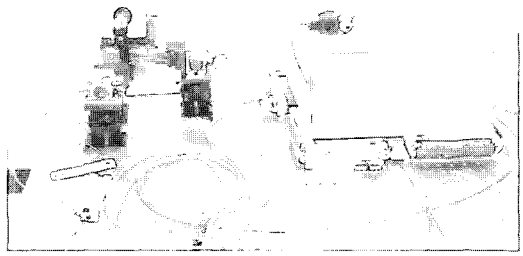

Fig. 1 Magnetic levitation stage

3. Control

3.1 Mechanical system modelling

In this section, we will derive the dynamics equation of the magnetic levitation stage. The coordinates of platen which is the levitation part of the stage is shown in Fig. 2. In the figure,

Σ_I and Σ_O represent inertial coordinates frame and object coordinates frame, respectively. Here $\eta_1=[x, y, z]^T$ and $\eta_2=[\phi, \theta, \psi]^T$denote the position and orientation vector with coordinates in the inertial coordinates frame.

$x_1=[u, v, w]^T$ and $x_2=[p, q, r]^T$denote the linear and angular velocity vector with coordinates in the object coordinate frame.

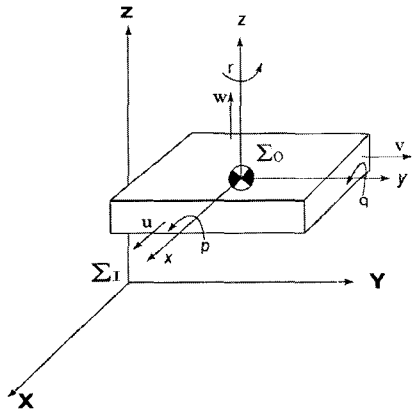

Fig. 2 Coordinates of the platen

The platen's movement path relative to the inertial frame is given by a velocity transformation

$$\dot{\eta}_1=J_1(\eta_2)k_1 \tag{1}$$

$$J_1(\eta_2)=\begin{pmatrix} c\psi c\theta & -s\psi c\phi+c\psi s\theta s\phi & s\psi s\phi+c\psi c\phi s\theta \\ s\psi c\theta & c\psi c\phi+s\phi s\theta s\psi & -c\psi s\phi+s\theta s\psi c\phi \\ -s\theta & c\theta s\phi & c\theta c\phi \end{pmatrix}$$

where J_1 is a transformation matrix which is related to the functions of the Euler angles: ψ(yaw), θ (pitch), ϕ(roll). In addition, c(·) and s (·) denote cos (·) and sin(·), respectively. The inverse velocity transformation can be written

$$x_1=J_1^{-1}(\eta_2)\,\dot{\eta}_1 \tag{2}$$

where J_1 is skew-symmetric matrix, i.e. $J_1^{-1}(\eta_2)=J_1^T(\eta_2)$. The object-fixed angular velocity vector $x_2=[p\ q\ r]^T$and the Euler rate vector $\dot{\eta}_2$ are related to a transformation matrix J_2 according to

$$x_2=J_2^{-1}(\eta_2)\,\dot{\eta}_2 \tag{3}$$

It should be noted that the angular velocity vector x_2 cannot be integrated directly to obtain actual angular coordinates. The angular velocity of the object-fixed reference frame with respect to the inertial frame is given by

$$\begin{aligned} x_2 &= \begin{pmatrix}\dot{\phi}\\0\\0\end{pmatrix}+C_{x,\phi}\begin{pmatrix}0\\\dot{\theta}\\0\end{pmatrix}+C_{x,\phi}C_{y,\theta}\begin{pmatrix}0\\0\\\dot{\psi}\end{pmatrix} \\ &= \begin{bmatrix}1 & 0 & -s\theta\\ 0 & c\phi & c\theta s\phi\\ 0 & -s\phi & c\theta c\phi\end{bmatrix} \end{aligned} \tag{4}$$

where $C_{x,\phi}$ and $C_{y,\theta}$ denote Euler angles respect to x and y axis.

From the above relations, we can formulate a suitable expression for the platen's kinetic energy

$$\begin{aligned} T &= \frac{1}{2}mx_1^Tx_1+\frac{1}{2}x_2^THx_2 \\ &= \frac{1}{2}m\dot{\eta}_1^T\dot{\eta}_1+\frac{1}{2}\dot{\eta}_2^T(J_2^{-1})^THJ_2^{-1}\dot{\eta}_2 \end{aligned} \tag{5}$$

and potential energy

$$V=mgz \tag{6}$$

Then we can compute the Lagrangian according to

$$L=T-V \tag{7}$$

Finally, applying the Lagrange equation

$$\frac{d}{dt}\left(\frac{\partial L}{\partial \dot{q}}\right)-\frac{\partial L}{\partial q}=u \tag{8}$$

we can get dynamics equation

$$M\ddot{q}+h_1+h_2(q,\dot{q})=u \tag{9}$$

$q=[x,y,z,\psi,\theta,\phi]^T$ is a state variables that represent the motion of system. $u=[F_x,F_y,F_z,\tau_x,\tau_y,\tau_z]^T$ is input vector which denotes forces and torques acting on the platen in the object-fixed frame. $M\in R^{6\times6}$ is an inertia matrix and $h_1\in R^{6\times1}$ and $h_2\in R^{6\times1}$ denote gravity and nonlinear terms.

3.2 Electrical system modelling

In this section we will consider an electrical dynamics for the levitation stage.

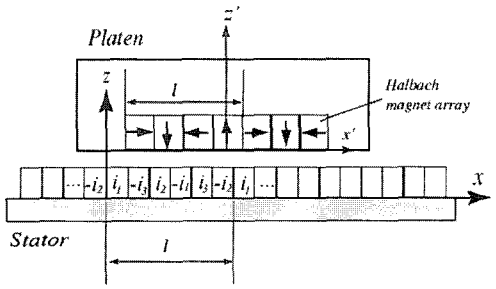

Fig. 3 Structure of the motor

The linear motor which employed in magnetic levitator is shown in Fig.3. Electrical dynamics of the linear motor can be derived from the Faraday's law. The voltage equations of three phase motor can be written

$$R_k i_k+\frac{d\lambda_k}{dt}=v_k \quad ,k=1,2,3. \tag{10}$$

where R_k is the resistance of winding and λ_k is the flux linkage of each phase winding. We can represent λ_k

$$\lambda_k(i_k,x,y,z)=\lambda_k(i_k,x-l,y,z) \tag{11}$$

We know that the flux linkage is periodic function with respect to x direction. Using chain-rule, we can get voltage equations as

$$R_k i_k+L_k(i_k,x,y,z)\frac{di_k}{dt}+E_{kx}+E_{ky}+E_{kz}=v_k \tag{12}$$

where

$$L_k=\frac{\partial\lambda_k}{\partial i_k},E_{kx}=\frac{\partial\lambda_k}{\partial x}\dot{x},E_{ky}=\frac{\partial\lambda_k}{\partial y}\dot{y},E_{kz}=\frac{\partial\lambda_k}{\partial z}\dot{z}$$

It is well known that co-energy is convenient quantity for expressing the electromagnetic force. We will introduce the co-energy to derive the electro-magnetic force generated by the current input. Derivative of co-energy can be defined as [7]

$$dW_c=\sum_{k=1}^{3}\lambda_k di_k+f_x dx+f_y dy+f_z dz \tag{13}$$

Integrating eq. (13) from $(0,0,0,0,0,0)$ to (i_1,i_2,i_3,x,y,z), then we can get

$$W_c=\sum_{k=1}^{3}\int_0^{i_k}\lambda_k(h,x,y,z)\,dh \tag{14}$$

Applying the chain-rule to eq. (14) and comparing with eq. (13), we have

$$\begin{aligned}&\lambda_k(i_k,x,y,z)=D_k W_c(i_1,i_2,i_3,x,y,z) \ ,k=1,2,3\\ &f_x(i_1,i_2,i_3,x,y,z)=D_4 W_c(i_1,i_2,i_3,x,y,z)\\ &f_y(i_1,i_2,i_3,x,y,z)=D_5 W_c(i_1,i_2,i_3,x,y,z)\\ &f_z(i_1,i_2,i_3,x,y,z)=D_6 W_c(i_1,i_2,i_3,x,y,z)\end{aligned} \tag{15}$$

where

$$D_1=\partial/\partial i_1, D_2=\partial/\partial i_2, D_3=\partial/\partial i_3$$
$$D_4=\partial/\partial x, D_5=\partial/\partial y, D_6=\partial/\partial z$$

Therefore, generating force f_x,f_y,f_z which has $2\pi/3$ phase difference can be obtained

$$\begin{aligned}f_x(i_1,i_2,i_3)&=\sum_{k=1}^{3}F_{xe}(i_k,x-\frac{l}{3}(k-1),y,z)\\ f_y(i_1,i_2,i_3)&=\sum_{k=1}^{3}F_{ye}(i_k,x-\frac{l}{3}(k-1),y,z)\\ f_z(i_1,i_2,i_3)&=\sum_{k=1}^{3}F_{ze}(i_k,x-\frac{l}{3}(k-1),y,z)\end{aligned} \tag{16}$$

where F_{xe},F_{ye},F_{ze} are

$$F_{ze}(i,x,y,z)=\int_0^i D_4\lambda(\eta,x,y,z)d\eta$$
$$F_{ye}(i,x,y,z)=\int_0^i D_5\lambda(\eta,x,y,z)d\eta \quad (17)$$
$$F_{xe}(i,x,y,z)=\int_0^i D_6\lambda(\eta,x,y,z)d\eta$$

Now we will consider flux linkage λ. Flux linkage on the one-phase winding can be written

$$\lambda(i,x,y,z)=\lambda_m(x,y,z)+\lambda_r(i,x,y,z) \quad (18)$$

where λ_m and λ_r reveal flux linkages generated by magnet array and current input into the stator, respectively. The flux linkage λ_m is decreased by increasing the height of platen and changed with its x direction movements. Then we have

$$\lambda_m(x,y,z)=\alpha(z)\lambda_a(x),\ 0<\alpha(z)\leq 1 \quad (19)$$

where $\alpha(z)$ is monotone decreasing function and $\lambda_a(x)$ is a periodic function with respect to x axis. The flux linkage λ_r can be represented

$$\lambda_r(x,y,z)=L(z)i \quad (20)$$

since the inductance L is only influenced by the height of platen. Now we can calculate E_x, E_y, E_z in eq.(12)

$$E_x(i,x,\dot{x},y,z)=\dot{x}\alpha(z)g_a(x)$$
$$E_y(i,x,y,\dot{y},z)=0 \quad (21)$$
$$E_z(i,x,y,z,\dot{z})=\dot{z}\left[\frac{d\alpha(z)}{dx}\{\lambda_a(x)\}+\frac{dL(z)}{dz}i\right]$$

where g_a denotes $g_a(x)=\dfrac{d\lambda_a(x)}{dx}$.

Substituting eq. (21) into eq. (12), we have

$$L(z)\frac{di_k}{dt}=-Ri_k-\dot{z}\left[\frac{d\alpha(z)}{dz}(\lambda_a(x))+\frac{dL(z)}{dz}i_k\right]-\dot{x}\alpha(z)g_a(x)+v_k \quad (22)$$

Forces generated by current input will be

$$f_x=\sum_{k=1}^{3}\alpha(z)g_a(x-\frac{l}{3}(k-1))i_k$$
$$f_z=\sum_{k=1}^{3}\left[\frac{d\alpha(z)}{dz}\lambda_a(x-\frac{l}{3}(k-1))i_k+\frac{1}{2}\frac{dL(z)}{dz}i_k^2\right] \quad (23)$$

We applied d-q transformation to eq. (22) and eq. (23). The d-q transformation was introduced to separate the stator current component that generates torque. Then, force equations and commutation in d-q frame do not contain the position dependence with respect to the stator. Therefore, non-linearity due to the trigonometric function in the model can be eliminated. Fig. 4 depicts d-q frame attached on the platen [6].

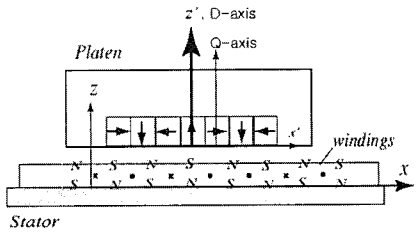

Fig. 4 d-q frame attached to the platen

It is shown that the q axis is orthogonal to the d axis and leads it by 90°. Applying d-q transformation, we have voltage equations on d-q axis from eq. (22)

$$L(z)\frac{di_d}{dt}=v_d-Ri_d-\dot{z}\left(\frac{d\alpha(z)}{dz}\lambda_d(x)+\frac{dL(z)}{dz}i_d\right)-\dot{x}\alpha(z)g_d(x)+\frac{2\phi}{l}L(z)\dot{x}i_q$$
$$L(z)\frac{di_q}{dt}=v_d-Ri_q-\dot{z}\left(\frac{d\alpha(z)}{dz}\lambda_q(x)+\frac{dL(z)}{dz}i_q\right)-\dot{x}\alpha(z)g_q(x)+\frac{2\phi}{l}L(z)\dot{x}i_d \quad (24)$$

Applying d-q transformation on eq. (23), we can get forces f_x, f_z

$$f_x=\frac{3}{2}\left[\frac{d\alpha(z)}{dz}\lambda_d(x)i_d+\frac{d\alpha(z)}{dz}\lambda_q(x)i_q+\frac{3}{4}\frac{dL(z)}{dz}(i_d^2+i_q^2)\right] \quad (25)$$
$$f_z=\frac{3}{2}\alpha(z)[g_d(x)i_d+\alpha(z)g_q(x)i_q]$$

3.3 The relations between forces and torques

Each motor generates vertical force for suspension against gravity, as well as horizontal force for driving a platen. Therefore, this stage can generate six degrees of freedom motion by the vertical and horizontal force. The relations between forces and torques on the platen can be described as

$$\begin{bmatrix} F_x \\ F_y \\ F_z \\ \tau_x \\ \tau_y \\ \tau_z \end{bmatrix} = \begin{bmatrix} 1 & 0 & 0 & 0 & 1 & 0 & 0 & 0 \\ 0 & 0 & 1 & 0 & 0 & 0 & 1 & 0 \\ 0 & 1 & 0 & 1 & 0 & 1 & 0 & 1 \\ 0 & b_1 & -c_2 & b_2 & 0 & b_3 & -c_4 & b_4 \\ c_1 & -a_1 & 0 & -a_2 & c_3 & -a_3 & 0 & -a_4 \\ -b_1 & 0 & a_2 & 0 & -b_3 & 0 & -a_4 & 0 \end{bmatrix} \begin{bmatrix} f_{1x} \\ f_{1z} \\ f_{2y} \\ f_{2z} \\ f_{3x} \\ f_{3z} \\ f_{4y} \\ f_{4z} \end{bmatrix} \quad (26)$$

where a_i, b_i, c_i $(i=1,2,3)$ denote the relations between horizontal forces on the stator and torques on the center of the mass of the platen. f_{ix} and f_{iz}, $(i=1,2,3,4)$ are x or y direction forces generating on the i th stators, respectively [7].

3.4 Control strategy

Based on the mechanical and electrical dynamics equation, we can design the control input to achieve desired movement of platen. In this section, we will propose the control algorithm to obtain control forces and torques (F, τ) in eq. (9) to move the platen from its initial posture to its desired one. Here we consider sliding mode control method which maintains robustness in the presence of a model uncertainty and an external disturbance.

Consider an inertia matrix in eq. (9) as

$$M = M^0 + \Delta M \quad (27)$$

where M^0 denotes estimated value and ΔM represents an error value between real value and estimated value. Let us assume each components of the inertia matrix can be estimated by its maximum value

$$| \Delta M_{ij}(q) | \leq \widehat{M}_{ij} \quad (28)$$

To compensate the gravity terms, we introduce control input

$$u = v_u + h_1 \quad (29)$$

where v_u denotes new control input and $h_1 = [0, 0, mg, 0, 0, 0]^T$ is a gravity compen -sation term.

Substituting eq. (27) and eq. (29) into eq. (9), then we have

$$\ddot{q} = M^{0^{-1}}(v_u + d) \quad (30)$$

$d(q, \dot{q}, \ddot{q}) = -\Delta M \ddot{q} - h_2$ denotes an estimated error and nonlinear terms of the dynamics equation. If we consider an absolute upper-limit value of $| \Delta M \ddot{q}_i | \leq \widehat{\rho}_i$, $| h_i(q, \dot{q})_i | \leq \widehat{h}_i$ then d can be estimated by scalar function $\widehat{d}(q, t)$

$$\widehat{d} = \max \ \omega_i \quad (31)$$

where $\omega_i = \widehat{\rho}_i + \widehat{h}_i$.

To achieve tracking performance, define the tracking errors as

$$e(t) = q - q_r, \ \dot{e}(t) = \dot{q} - \dot{q}_r \quad (32)$$

where q and q_r denote current state variable and desired state variable, respectively.

Here we introduce switching surface

$$\sigma(t) = \dot{e} + \Lambda e \qquad (33)$$
$$\Lambda = diag(\alpha_1, \alpha_2, \cdots, \alpha_6)$$

where Λ is a positive definite matrix.

The control problem is to derive control input u which guarantees $\sigma(t) \to 0$ and preserve states $q, \dot{q}$ on the sliding surface. To derive such a control input, we can consider Lyapunov function candidates

$$V = \frac{1}{2}\sigma^T\sigma \qquad (34)$$

Time differentiation of eq. (34) is

$$\begin{aligned} \dot{V} &= \sigma^T\dot{\sigma} \\ &= \sigma^T(\ddot{e} + \Lambda\dot{e}) \\ &= \sigma^T(M^{o^{-1}}v_u + M^{o^{-1}}d - \ddot{q}_r + \Lambda\dot{e}) \end{aligned} \qquad (35)$$

Let's consider new control input as

$$v_u = M^o(\ddot{q}_r - \Lambda\dot{e} - K\frac{\sigma}{\|\sigma\|}) \qquad (36)$$

where $K > \|M^{0^{-1}}\| \cdot d$

Then, we have

$$\dot{V} = -\|\sigma\|(K \pm M^{o^{-1}}d) \le 0 \qquad (37)$$

Therefore, $\sigma(t) \to 0$ was achieved from eq. (34) and eq. (36) as $t \to \infty$. We can see that $\sigma(t) \to 0$ means stabilization of error variable because it makes stable error equation $\dot{e} = -\Lambda e$ under the condition of the new control input eq. (36). Finally, the control input to achieve configuration control purpose can be obtained from eq. (29) and eq. (36)

$$u = M^o(\ddot{q}_r - \Lambda\dot{e} - K\frac{\sigma}{\|\sigma\|}) + h_1 \qquad (38)$$

3.5 Simulation results

To illustrate the effectiveness of the proposed control scheme, we present a simulation result for an magnetic levitation stage. In the simulation, initial value q_0 and desired value q_r are $(0, 0, 250\mu m, 0.01, 0.02, 0.03)^T$ and $(0.03, 0.03, , 350\mu m, 0, 0, 0)^T$ respectively. We set the parameters as $m = 5.47[kg]$, $g = 9.8[m/s^2]$, $\Lambda = diag[3, 3, 3, 3, 3, 3]$. Estimated value M^o was considered to 70% of the diagonal terms of inertia matrix M. In the simulation we introduced smoothing unction

$$u = M^0(\ddot{q}_r - \Lambda\dot{e} - K\frac{\sigma}{\|\sigma\| + \delta}) + h_1, \quad \delta = 0.05$$

to remove chattering phenomenon. The numerical simulation results for the configuration control are shown in Fig. 5, Fig. 6 and Fig. 7.

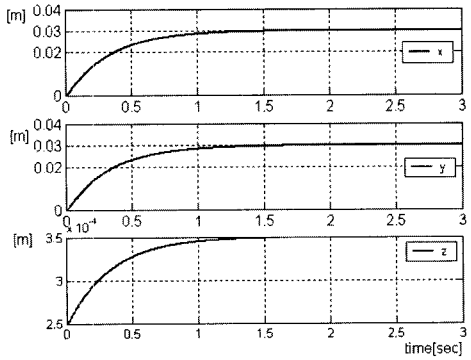

(a) x, y, z

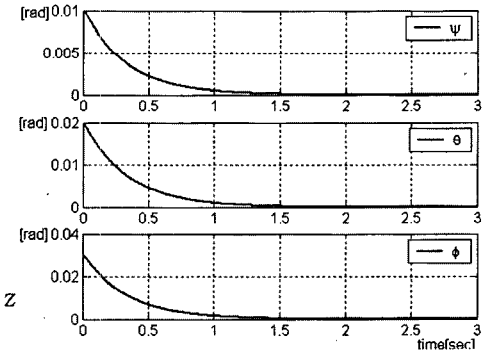

(b) ϕ, θ, ψ

Fig. 5 Time evolution of states

Fig. 5 shows the time evolution of state variables. Fig. 6 depicts control input generated by proposed control strategy. In the each figure, the upper graph indicates the enlarged time axis (from 0 to 0.5 sec.) of under result.

In Fig.6, y axis values on (a), (b), (c) and (d), (e), (f) are forces [$kg \cdot m/s^2$] and torques [$kg \cdot m^2/s^2$], respectively.

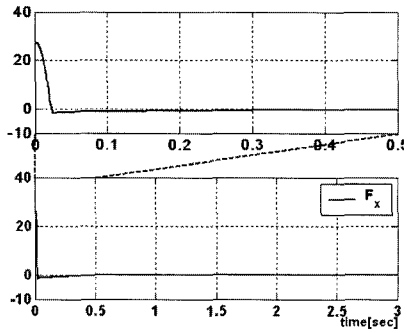

(a) F_x

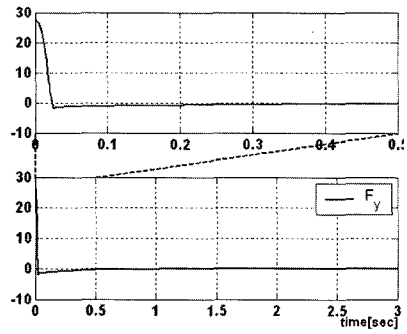

(b) F_y

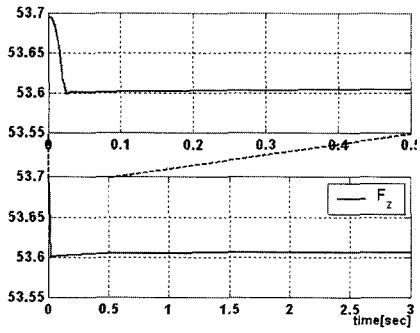

(c) F_z

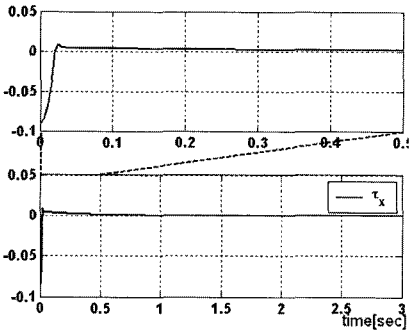

(d) τ_x

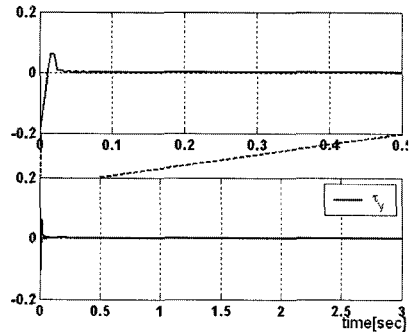

(e) τ_y

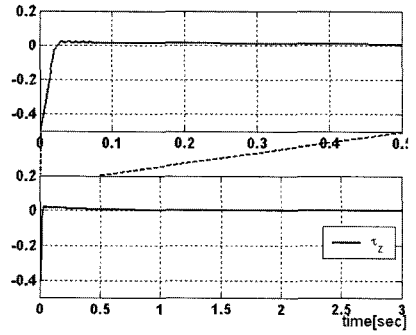

(f) τ_z

Fig. 6 Control inputs

Fig. 7 denotes switching surfaces. To show the details, we omit the results after 1 second. The reaching time to the sliding surface was 0.04 [sec]. If the states are arrived at the switching surfaces, the states will maintained on the sliding surface by its switching action.

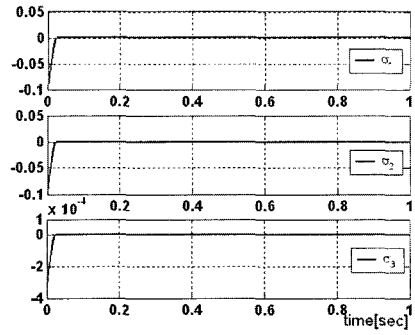

(a) $\sigma_1, \sigma_2, \sigma_3$

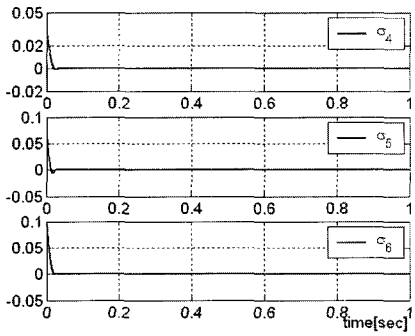

(b) $\sigma_4, \sigma_5, \sigma_6$

Fig. 7 Switching surfaces

From the simulation results, we see that the desired control purpose was achieved by proposed control scheme.

4. Conclusions

In this paper, we addressed configuration control for the magnetic levitation stage. We derived dynamic equation of the platen and electrical system dynamics using co-energy. We also proposed control strategy which can control its position and posture. To derive the control input, we applied sliding mode control method which can maintain the performance and stability robustness for model uncertainty. Finally, we verified an effectiveness of the control algorithm by numerical simulation.

References

[1] V. I. Utkin, "Variable structure systems with sliding mode", IEEE Trans. Automation and Control, vol. AC-22, pp. 212-222, 1977.

[2] M. Y. Chen, M. J. Wang, and L. C. Fu, "A Novel dual axis repulsive maglev guiding system with permanent magnet: modeling and controller design", IEEE/ASME Trans. on mechatronics, vol. 8, no. 1, pp. 77-86, 2003.

[3] D. Cho, Y. Kato and D. Spilman, "Sliding mode and classical controller in magnetic levitation," IEEE control systems, pp. 42-48, 1993.

[4] W. J. Kim, "High-Precision planar magnetic levitation", Ph. D. Dissertation, Massachusetts Institute of Technology, 1997.

[5] M. L. Holmes, R. Hocken and D. L. Trumper, "The long range scanning stage: a novel platform for scanned probe microscopy", *Precision Engineering*, vol. 24, no. 3, pp. 191-209, 2000.

[6] S. Mittal, C. H. Menq, "Precision motion control of a magnetic suspension actuator using a robust nonlinear compensation scheme", *IEEE/ASME Transactions on Mechatronics*, vol. 2, no. 4, pp. 268-280, 1997.

[7] T. K. Nam, Y. J. Kim, "A study on the modelling for the control of magnetic levitation", Journal of KOSME, vol. 27, no. 3, pp. 862-871, 2003.

저 자 소 개

남택근 (南澤槿)

1968년10월생. 1986년 한국해양대학교 기관공학과 졸업. 1996년 한국해양대학교 기관공학과 대학원 졸업(공학석사). 2001년 동경공업대학 제어공학과 졸업(공학박사). 2002년 4월~2003년 8월 한국전기연구원 선임연구원. 현재 목포해양대학교 기관시스템공학부 전임강사

김용주 (金容柱)

1953년 11월생. 1975년 서울대학교 전기공학과 졸업. 1987년 미국 Rensselaer Polytechnic Institute(R.P.I) 대학원 졸업(공학박사). 현재 한국전기연구원 기기제어응용그룹 그룹장 (책임연구원)

전정우 (全廷佑)

1971년 11월생(음). 1994년 영남대학교 전기공학과 졸업. 1996년 영남대학교 전기공학과 대학원 졸업(공학석사). 현재 한국전기연구원 기기제어응용그룹 선임연구원.